Biochemistry

 Volume 35, Number 14 April 9, 1996

Articles

Interaction of a DNA-Threading Netropsin−Amsacrine Combilexin with DNA and Chromatin†

Catherine Bourdouxhe-Housiaux,‡ Pierre Colson,‡ Claude Houssier,‡ Michael J. Waring,§ and Christian Bailly*,‖

Laboratoire de Chimie Macromoléculaire et Chimie Physique, Université de Liège, Sart-Tilman (B6), Liège 4000, Belgium, Department of Pharmacology, University of Cambridge, Tennis Court Road, Cambridge CB2 1QJ, U.K., and INSERM U124, Institut de Recherches sur le Cancer, Place de Verdun, 59045 Lille Cedex, France

Received November 28, 1995; Revised Manuscript Received February 7, 1996⊗

ABSTRACT: Combilexins are a group of DNA ligands having a sequence-specific minor groove binding element combined with an intercalating chromophore which stabilizes the DNA complex and can interfere with topoisomerases. In this study, complementary methods of spectroscopy (absorption, circular dichroism, electric linear dichroism) and biochemistry (viscometry, footprinting) have been applied to explore the nature of the complex formed between a new amsacrine-4-carboxamide−netropsin combilexin and DNA or chromatin. Collectively, the structural and kinetic data concur that the conjugate threads through the DNA double helix so as to intercalate its acridine chromophore, leaving the netropsin moiety and the methanesulfonanilino group positioned within the minor and major grooves of the double helix, respectively. The hybrid retains the AT selectivity conferred by the netropsin moiety. The threading-type intercalation process, evidenced by stopped-flow measurements, is affected when the DNA is wrapped around histones. The composite drug can bind to both the DNA linker segments and the nucleosomal cores in chromatin though, unlike its constituents, it antagonizes the salt-induced condensation of chromatin. As far as its mode of binding to DNA is concerned, the netropsin−amsacrine hybrid molecule exhibits structural features reminiscent of the antitumor antibiotics nogalamycin and pluramycin. The design of DNA-threading combilexins provides an original route for the development of sequence-specific ligands capable of forming stable complexes with DNA.

Progress in cancer research over the last 20 years has led to the inescapable conclusion that neoplasia is a malady of genes (Bishop, 1987). The large number of malignancies that do not respond to chemotherapy underline the need to develop safe and effective antitumor drugs. Although several potent antitumor drugs do not interact with nucleic acids (e.g., taxol), the steady accumulation of evidence that the malignant tranformation of a cell—be it a cell of the blood, lung, or brain—is due to an alteration of particular genes calls clearly for the development of DNA-interacting substances. Moreover, among macromolecules DNA is probably the best structurally characterized target, thus making it an attractive receptor for drug design (Hurley, 1988, 1989; Nielsen, 1991; Lown, 1995).

Three major aspects of the binding of drugs to DNA could be expected to influence their biological activity: (i) mode

† This work was done under the support of research grants (to C.B.) from the INSERM and the ARC, (to C.H. and P.C.) from the FRFC convention 2.4501.91 and the FNRS, and (to M.J.W.) from the Wellcome Trust, CRC, AICR, and Sir Halley Stewart Trust. Support by the convention INSERM-CFB is acknowledged. C.B.-H. is the recipient of an IRSIA fellowship.

* Address correspondence to this author.
‡ Université de Liège.
§ University of Cambridge.
‖ INSERM U124.

⊗ Abstract published in *Advance ACS Abstracts,* March 15, 1996.

0006-2960/96/0435-4251$12.00/0

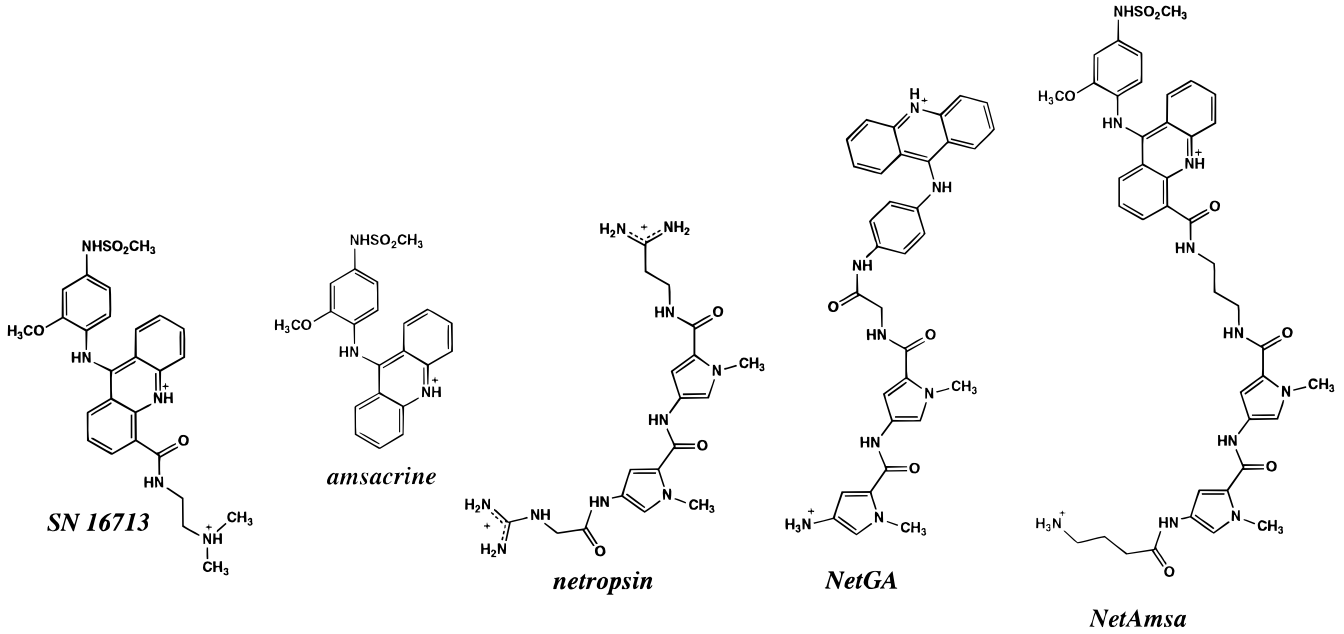

FIGURE 1: Structure of netropsin, amsacrine (*m*-AMSA), the amsacrine-4-carboxamide SN 16713, the netropsin−anilinoacridine hybrid NetGA, and the netropsin−amsacrine hybrid NetAmsa.

of interaction with the double helix, (ii) sequence specificity of binding, and (iii) kinetics of association/dissociation. It has recently become clear that in addition to considering these three critical levels of DNA recognition it is also important to examine the interaction of drugs with complexes between DNA and gene-regulatory proteins (e.g., transcription factors, topoisomerases) as well as chromatin structures which more closely model the arrangement of DNA *in vivo*. The potential design of drugs capable of recognizing specifically defined sequences according to some well-defined geometry is becoming a reality (Kopka & Larsen, 1992; Geierstanger et al., 1994; Chen & Lown, 1994). A no less important issue is to understand how the presence of proteins bound to DNA might affect the binding/recognition of drugs. The biological activity of most clinically used antitumor agents certainly depends on their capacity to bind to nucleic acids, but in most cases their pharmacological effects are critically dependent upon their capacity to modulate the activities of DNA-interacting proteins (in particular, topoisomerases) and to influence nucleic acid condensation (Kapuscinski & Darzynkiewicz, 1984, 1986; Schröter et al., 1985; Bartkowiak et al., 1989; Ralph et al., 1993; Powis & Workman, 1994; Chen & Liu, 1994).

With these parameters in mind, we postulated that the combination of a DNA minor groove binding agent with an intercalating chromophore should furnish potentially useful antitumor agents. Hybrid molecules—named combilexins—were designed with the rationale that the pseudopeptide may support the DNA sequence selectivity and that the attached intercalating chromophore may provide DNA binding affinity, additionally contributing to interference with topoisomerases and perhaps facilitating the cellular penetration of the hybrid molecule (Bailly & Hénichart, 1991, 1994). Most combilexins designed so far (e.g., distamycin−ellipticine, netropsin−acridine) have been shown to be capable of recognizing specific sequences in DNA and to modulate topoisomerase activities in a fashion which correlates with their antitumor activities (Bailly et al., 1990, 1992a,b, 1993, 1994; Bourdouxhe et al., 1992; Fossé et al., 1994; Plouvier et al., 1994; Riou et al., 1995; René et al., 1995). In addition to sequence-selective binding and inhibition of topoisomerase activities, it may be profitable to design hybrid drugs which form slowly dissociating complexes with DNA. Various studies have highlighted the importance of the kinetic stability of drug−DNA complexes as a determinant of biological activity (Müller & Crothers, 1968; Wakelin & Waring, 1980; Feigon et al., 1984; Chaires et al., 1985; Chaires, 1990; Denny & Wakelin, 1986, 1990; Wilson & Tanious, 1994). A hybrid molecule which dissociates slowly from DNA with a long residence time at particular nucleotide sequences should more efficiently block the activity of gene-regulatory enzymes.

To this end, we now report molecular aspects of the interaction of a second generation hybrid ligand with DNA and chromatin. The new conjugate consists of a minor groove-binding netropsin-like moiety attached to an intercalating chromophore structurally related to the antileukemic drug amsacrine (Figure 1. This netropsin−amsacrine hybrid, henceforth called NetAmsa, differs from the netropsin−anilinoacridine derivative NetGA (Figure 1) previously studied (Bailly et al., 1990, 1992a) in three major structural respects. First, it bears a positively charged terminal side chain which contributes significantly to the AT selectivity of such ligands (Bailly et al., 1994). Second, the new hybrid retains the *m*-methoxy and methanesulfonamide substituents on the anilino ring which constitute key elements for the interference with topoisomerases, the maintenance of redox properties, and the biological properties of amsacrine. Third, and that is the essential point, the netropsin moiety is connected to the acridine ring via a 4-carboxamide side chain whereas it was previously attached directly to the anilino group. By modifying the connector between the two DNA-binding units, we sought to modify the mechanism of binding to DNA. Linkage of a carboxamide side chain to position 4 of the acridine ring of amsacrine has earlier been shown to convert the drug from a classical intercalator to a threading intercalator (Denny & Wakelin, 1986; Bailly et al., 1992c). By extension, the substitution of the anilinoacridine moiety

of the hybrid NetGA with an amsacrine-4-carboxamide moiety should lead to an obligate DNA-threading combilexin capable of forming slow-dissociating complexes with DNA. It needs to be noted that before synthesizing this conjugate we investigated the possibility of mutual interference between netropsin and amsacrine or its 4-carboxamide derivative SN 16713 (Figure 1) and showed that DNA can accommodate a minor groove binder and an intercalating drug—be it a threading or a classical intercalator—in close proximity (Bourdouxhe et al., 1995).

We have applied a range of spectroscopic and biochemical techniques to build up a complete description of the structure of the nucleic acid−NetAmsa complex. These have included attempts to delineate the role of the netropsin moiety as opposed to the amsacrine chromophore in the interaction of the hybrid with both DNA and chromatin. Kinetic data were determined along with an assessment of the effects on chromatin condensation. These studies show that the netropsin−amsacrine hybrid NetAmsa does behave as a sequence-specific DNA-threading combilexin.

MATERIALS AND METHODS

Drugs and Chemicals. Netropsin was purchased from Serva (Heidelberg, Germany). The amsacrine-4-carboxamide derivative SN 16713 was obtained by courtesy of Prof. W. A. Denny (University of Auckland, New Zealand). Amsacrine (*m*-AMSA), Hoechst 33258, DAPI, and ethidium bromide were purchased from Sigma Chemical Co. (La Verpillière, France). The synthesis of the hybrid molecule NetAmsa will be reported later together with the biological studies. Briefly, the 4-carboxamide side chain was introduced onto the acridine ring before addition of the substituted aniline moiety (Wakelin et al., 1990) by reacting [(*tert*-butyloxycarbonyl)amino]propylamine with 9-chloroacridine-4-carbonyl chloride. Then the bispyrrole block which mimics the antibiotic netropsin was coupled with the amsacrine-4-carboxamide moiety via the agency of dicyclohexylcarbodiimide and hydroxybenzotriazole. Published chemical procedures were used to synthesize 4-[[4-(aminobutyramido)-1-methylpyrrol-2-ylcarbonyl]amino]-1-methylpyrrole-2-carboxylic acid (Bailly et al., 1989). The N-terminal BOC protecting group was removed with HCl−acetic acid, and the final purification was accomplished by flash chromatography. Drug concentrations were determined spectroscopically in 10 mm path-length quartz cuvettes using the following molar extinction coefficients (in M^{-1} cm^{-1}): 21 500 at 296 nm for netropsin, 12 000 at 434 nm for amsacrine; 42 000 at 338 nm for Hoechst 33258; 23 000 at 342 nm for DAPI; 5700 at 480 nm for ethidium bromide; 12 900 at 442 nm for SN 16713; and 13 000 at 440 nm for NetAmsa.

Biochemicals. The various natural DNAs and synthetic polynucleotides were purchased from Sigma Chemical Co. Calf thymus (CT) DNA (highly polymerized sodium salt) was deproteinized twice with sodium dodecyl sulfate (SDS) and precipitated with ethanol (final protein content <0.2%). All nucleic acids were dialyzed against 1 mM sodium cacodylate buffer, pH 6.5. DNA concentrations were determined, applying the molar extinction coefficients given in the literature (Wells et al., 1970). The preparation of chicken erythrocyte chromatin fragments followed the procedures described earlier (Hagmar et al., 1989). In the ionic strength conditions used for electric linear dichroism measurements (1 mM cacodylate, pH 6.5), chromatin (10−80 nucleosomes long) is mostly present as the 10 nm fiber. Plasmids pBS and pKMΔ-98 were isolated from *Escherichia coli* by a standard sodium dodecyl sulfate−sodium hydroxide lysis procedure and purified by banding in CsCl−ethidium bromide gradients. The plasmids were cut with *Eco*RI, treated with alkaline phosphatase, and then labeled at the 5′-end using T4 polynucleotide kinase (Pharmacia) and [γ-^{32}P]ATP (6000 Ci/mmol, New England Nuclear). The linear labeled plasmid was further digested with *Pvu*II to generate the singly end-labeled DNA fragment which was then purified by preparative nondenaturing polyacrylamide gel electrophoresis.

Viscosity measurements were carried out in a capillary viscometer submerged in a 45 L water bath which was maintained at 25 ± 0.1 °C (Révet et al., 1971; Waring & Henley, 1975). Flow times were measured at least in triplicate to an accuracy of ±0.1 s with a stopwatch, and the average time was calculated. The pUC12 plasmid DNA was isolated by a standard sodium dodecyl sulfate−sodium hydroxide lysis procedure and purified by banding twice in CsCl−ethidium bromide gradients. This procedure yields pure covalently closed circular supercoiled DNA suitable for viscosity measurements. Aliquots (1−5 μL) of the test drug solution (1−2 mM) were titrated directly into the viscometer containing 2 mL of a solution of the plasmid at various concentrations (125−250 μM). After each addition, the solutions were carefully mixed with a small flow of air through the dilution bulb of the viscometer and the flow times measured. Experiments were conducted in buffer containing 10 mM Tris-HCl (pH 7.0) and 10 mM NaCl. Unwinding angles were estimated by reference to an unwinding angle of 26° for ethidium bromide (Wang, 1974) used as a control.

Absorption Spectroscopy. Absorption spectra were recorded on a Perkin-Elmer Lambda 5 spectrophotometer using a 10 mm optical path length. Titrations of the drugs with DNA, covering a large range of drug/DNA−phosphate ratios (D/P), were performed by adding aliquots of a concentrated DNA (or chromatin) solution to a drug solution at constant ligand concentration (10 μM). Melting temperature studies were performed using a Uvikon Kontron 810/820 spectrophotometer. The cuvette was heated by circulating water, and the absorbance at 260 nm was measured over the range 20−95 °C with a heating rate of 1 °C/min. Drug−DNA complexes were prepared by adding stock drug solutions to a 50 μM CT DNA solution in 0.1 SSC (1.5 mM sodium citrate, 15 mM sodium chloride) buffer to obtain the desired D/P ratio. The "melting" temperature T_m was taken as the midpoint of the hyperchromic transition.

Fluorescence intensity was determined using a Kontron SFM25 spectrofluorometer. All measurements were made in a 10 mm path-length cuvette with 0.01 M ionic strength buffer (9.3 mM NaCl, 2 mM sodium acetate, 0.1 mM EDTA) using 20 μM DNA and 2 μM ethidium bromide or Hoechst 33258 or DAPI (Baguley et al., 1981). Small aliquots of the test ligand (2−5 μL) from a concentrated solution were added to 3 mL of a fluorophore−DNA solution. The relative fluorescence intensity was recorded after 5 min of equilibration. The DNA−ethidium complex was excited at 546 nm and the fluorescence measured at 595 nm. For Hoechst 33258 and DAPI, excitation was at 353 and 360 nm, and fluorescence was measured at 465 and 450 nm, respectively.

Circular dichroism (CD) measurements were recorded on a Jobin-Yvon CD6 dichrograph. Solutions of drugs and/or nucleic acids were scanned in 0.5 cm quartz cuvettes. Measurements were made by progressive addition of DNA or chromatin to a pure ligand solution to yield the desired drug/DNA ratios. Five scans were accumulated and automatically averaged. Results are expressed in terms of molar circular dichroism $\Delta\epsilon = \Delta A/lc$, where ΔA is the circular dichroism amplitude, l the cell path length, and c the total ligand concentration.

Electric linear dichroism (ELD) measurements were performed using a computerized optical measurement system built by C. Houssier (Houssier & O'Konski, 1981). The procedures outlined previously were followed (Houssier, 1981). The optical setup incorporating a high sensitivity T-jump instrument equipped with a Glan polarizer was used under the following conditions: bandwidth 3 nm, sensitivity limit 0.001 in $\Delta A/A$, and response time 3 ms. Equations used for the calculation of the different parameters have been reported (Houssier, 1981; Bailly et al., 1992d). All experiments were conducted at 20 °C with a 10 mm path-length Kerr cell having 1.5 mm electrode separation, in 1 mM sodium cacodylate buffer, pH 6.5. The DNA samples were oriented under an electric field strength of 13 kV/cm, and the drug under test was present at 10 μM together with the DNA or polynucleotide at 100 μM unless otherwise stated.

To investigate the geometry of drug binding to DNA by ELD, the reduced dichroism $\Delta A/A$ of a ligand−DNA complex measured in the ligand absorption band must be analyzed with respect to the reduced dichroism measured for the same DNA or polynucleotide at 260 nm in the absence of drug, $(\Delta A/A)^{DNA}$. The dichroism ratio DR is defined as follows: $DR = [(\Delta A/A)^{ligand-DNA}]/[(\Delta A/A)^{DNA}]$. The numerator refers to the reduced dichroism of the drug−DNA complex measured at the absorption maximum of the ligand bound to DNA. The denominator is always negative under the experimental conditions used. The dichroism ratio is expected to be +1 if the transition moment of the drug chromophore is parallel to the DNA bases, as in the case of complete intercalative binding. For groove binders, the angle between the double helical axis and the long axis of the chromophore lies below 54°, which gives rise to positive dichroism and thus to a negative DR value. Under these conditions, the reduced dichroism ratios for any given drug−DNA and drug−polynucleotide complexes can be mutually compared with good relative accuracy, independent of the polymer size (Bailly et al., 1992d; Colson et al., 1995).

Kinetic measurements were conducted with a Bio-Logic SFM-3 stopped-flow spectrometer coupled to Bio-Kine V3.0 software for data acquisition and analysis. Single-wavelength kinetic records of voltage versus time were collected and converted to absorbance. Typically, 8−10 runs were collected and averaged by the computer to improve the signal-to-noise ratio. Dissociation reactions were monitored by mixing equal volumes (100 μL) of a DNA−drug complex and a 1% SDS solution according to the method of Müller and Crothers (1968). The wavelength used to carry out the measurements was chosen as the maximum of the drug absorption band in SDS solution. Checks were carried out to make sure that no time-resolvable changes occurred on mixing free drug solutions with SDS. Therefore, we can assume that the optical changes observed in the stopped-flow spectrophotometer are not related to processes associated with absorption of the drug into the surfactant micelles but reflect the SDS-induced dissociation of the drug−DNA complexes. The dead time of the instrument was 3 ms. Digitized traces were fitted to multiple exponentials by a least-squares fitting procedure. The dissociation of the drugs from chromatin was induced by increasing the ionic strength (salt jump).

DNase I footprinting experiments were performed essentially according to published protocols (Low et al., 1984; Bailly & Waring, 1995a). Reactions were conducted in a total volume of 10 μL. Samples (3 μL) of the labeled DNA fragment were incubated with 5 μL of buffer solution (10 mM Tris-HCl, 10 mM NaCl, pH 7.0) containing the desired drug concentration. After 30−60 min incubation at 37 °C to ensure equilibration, the digestion was initiated by addition of 2 μL of a DNase I solution so as to yield a final enzyme concentration of about 0.01 unit/mL. The extent of digestion was limited to less than 30% of the starting material so as to minimize the incidence of multiple cuts in any strand ("single-hit" kinetic conditions). Optimal enzyme dilutions were established in preliminary calibration experiments. After 3 min, the reaction was stopped by addition of 3 μL of an 80% formamide solution containing tracking dyes. Samples were heated at 90 °C for 4 min and chilled in ice for 4 min prior to electrophoresis.

Electrophoresis and Autoradiography. DNA cleavage products were resolved by electrophoresis under denaturing conditions in polyacrylamide gels (0.3 mm thick, 8% acrylamide containing 8 M urea). Electrophoresis was performed for about 2 h at 60 W in TBE buffer: 89 mM Tris base, 89 mM boric acid, and 2.5 mM Na_2 EDTA, pH 8.3. Gels were soaked in 10% acetic acid for 15 min, transferred to Whatman 3MM paper, dried under vacuum at 80 °C, and then analyzed on the phosphorimager.

Quantitation by Storage Phosphor Technology Autoradiography. Photostimulatable storage phosphor imaging plates (Kodak storage phosphor screens obtained from Molecular Dynamics) were pressed flat against dried sequencing gels and exposed overnight at room temperature. A Molecular Dynamics 425E PhosphorImager was used to collect all data. Base-line-corrected scans were analyzed by integrating all the densities between two selected boundaries using the ImageQuant version 3.3 software. Each resolved band on the autoradiograph was assigned to a particular bond within the DNA fragment by comparison of its position relative to the sequencing standards generated by treatment of the DNA with formic acid (G+A) track followed by piperidine-induced strand cleavage at the modified purine nucleotides.

RESULTS AND DISCUSSION

Characterization of the Hybrid−DNA Interaction. Initial attempts to determine DNA-binding isotherms were made by titrating measured quantities of a stock solution of the hybrid drug into a known volume of calf thymus DNA solution and monitoring the resulting changes in the absorption spectrum of the ligand. A bathochromic shift and hypochromism are observed when the hybrid is added to DNA, but there is no isosbestic point, indicating that there exists more than one spectroscopically distinct type of binding (spectra not shown). Figure 2 shows the variation of the absorption at 435 nm in the presence of either DNA

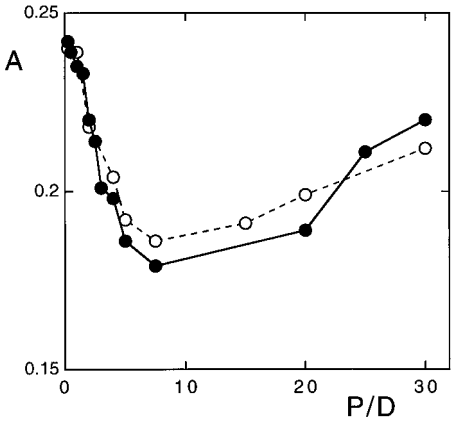

FIGURE 2: Variation of the absorbance at 435 nm with increasing amount of NetAmsa bound to calf thymus DNA (●) or chromatin (○) in 1 mM sodium cacodylate buffer, pH 6.5.

or chromatin, under the low ionic strength conditions (1 mM Na^+) chosen to meet the requirements of the electric linear dichroism experiments (see below). In both cases, the absorption first decreases up to a DNA−phosphate/drug ratio (P/D) of about 10 and then increases to reach a maximum for P/D ≥ 30. Under such conditions attempts to estimate the binding constant from conventional Scatchard analysis are doomed to failure. Given the absence of an isosbestic point and the difficulty in distinguishing between free and bound molecules, the spectrophotometric method is strictly not applicable.

Two alternative procedures were tried to estimate the strength of the hybrid−DNA interaction. First, we determined the ability of the test drugs to alter the thermal denaturation profile of DNA. T_m values corresponding to the helix-to-coil transition of calf thymus DNA measured in the presence of the hybrid and the parent compounds at different drug−DNA ratios are collated in Table 1. Netropsin stabilizes the duplex structure much more strongly than does amsacrine-4-carboxamide or the hybrid. The slightly higher stabilization of the DNA double helix by SN 16713 compared to amsacrine likely reflects the interaction of the aminoalkylcarboxamide side chain with the DNA. Second, we employed fluorescence spectroscopy to examine the abilities of the test drugs to compete with a DNA-binding ligand for available binding sites. In these experiments the fluorescent probes used were the intercalating drug ethidium bromide and the two AT-selective minor groove binders Hoechst 33258 and DAPI. All three probes are highly fluorescent in the presence of DNA. The fluorescence of the molecules free in solution is sufficiently small to neglect. The concentration of drug required to reduce by 50% the fluorescence of the DNA−fluorophore complex (Q_{50}) is listed in Table 1. Netropsin reduces more efficiently the fluorescence of the minor groove binder−DNA complexes than that of the ethidium−DNA complex. The opposite is observed for the intercalating drug amsacrine. The finding that SN 16713 efficiently diminishes the fluorescence of both the intercalator−DNA and the minor groove binder−DNA complexes is consistent with its threading mechanism of interaction (which involves both intercalation and groove binding). The behavior of the hybrid ligand is very different from that of amsacrine but is quite similar to that of SN 16713. Caution must be exercised in interpreting the fluorescence data because both drug displacement and quenching can contribute to the observed reduction of fluorescence intensity. However, the results are entirely consistent with the belief that the two moieties of the hybrid molecule participate in the binding reaction. When the modes of binding of the test ligand and the fluorescent reporter molecule are identical, such competitive fluorescence measurements can be used to calculate intrinsic association constants. But when the binding modes are dissimilar, as is the case here with our bifunctional ligand, the fluorescence assay can only provide a relative scale of affinity. The comparable effects of the hybrid and SN 16713 on the T_m of the DNA double helix and in the fluorescence assay, as well as their comparable dissociation kinetics (see below), suggest that the affinity constant for NetAmsa must be little different from that of its amsacrine-4-carboxamide parent, i.e., in the order of $\sim 10^6$ M^{-1}.

Geometry of the Hybrid−DNA Complex. (A) Viscometry. Good evidence for an intercalative mode of binding derives from the conformational changes in the DNA molecules that accompany insertion of the drug chromophore between its base pairs. A reduction in the winding angle of the B-type double helix by 10−26° depending on the chromophore characterizes the intercalation of a drug into DNA (Waring, 1970). We performed viscometric experiments to observe the effect of binding of the hybrid on the superhelix density of covalently closed circular plasmid DNA (Figure 3). In the viscometric titration, the equivalence point corresponds to the binding ratio where the original negative supercoils of the plasmid are just balanced by the cumulative ligand-induced unwinding, i.e., when the superhelix density is zero. With the hybrid as well as with the control compounds, the drug concentration required to reach the equivalence point was determined starting from different DNA concentrations. This procedure was used to construct equivalence plots such as that shown in the inset of Figure 3 which enables an accurate estimation of the helix unwinding angle (Table 1). The angle calculated for SN 16713 (18°) is consistent with those previously reported for anilinoacridine derivatives and for amsacrine in particular (Waring, 1976; Wakelin et al., 1990). The amount of hybrid molecule required to reach equivalence is about 2-fold greater than the amount of SN 16713 required to reach the same point. As a consequence, the calculated unwinding angle for NetAmsa (9°) is half that of the amsacrine-4-carboxamide derivative. The same situation was observed with the distamycin−ellipticine hybrid ligands previously studied: the unwinding produced by the parent ellipticine moiety was about twice that produced by the hybrid (Bailly et al., 1994). At least three explanations can be postulated to explain why the present hybrid is half as effective as SN 16713 in promoting DNA unwinding. First, the low unwinding angle can result from the coexistence of two hybrid drug populations, only one having the amsacrine moiety fully intercalated. Second, the acridine moiety of the hybrid might adopt a particular configuration within the double helix that differs from the classical intercalation model and would only partially unwind the double helix (e.g., insertion into a locally kinked DNA site). Third, the unwinding induced by the intercalating ring could be accompanied by an overwinding produced by the minor groove binding moiety. This latter suggestion is plausible because netropsin has been reported to engender a weak but noticeable overwinding of the double helix (Snounou & Malcolm, 1983), and a tendency to induce positively supercoiled DNA has also been noticed with distamycin (Bailly

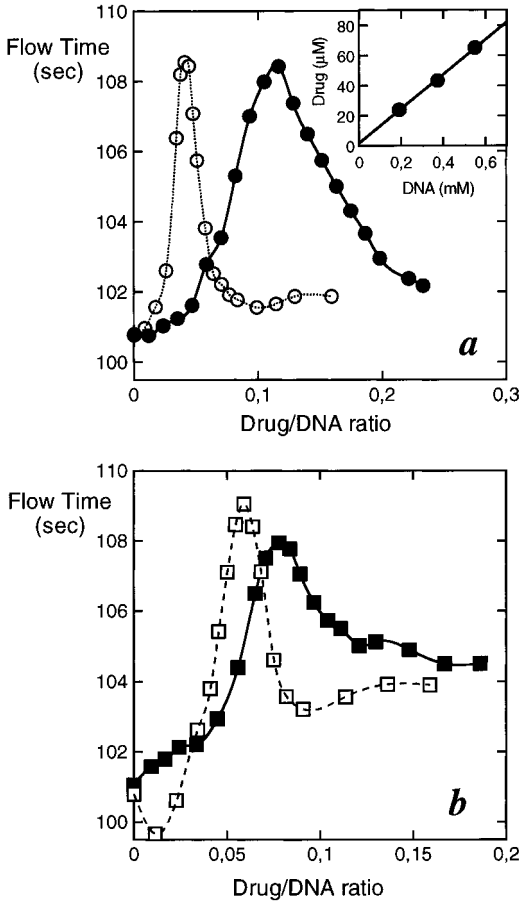

FIGURE 3: Viscometric titrations of pUC12 closed circular duplex DNA with (a) ethidium bromide (○) and NetAmsa (●) and (b) SN 16713 in the absence (□) and presence (■) of an equimolar concentration of netropsin. The flow time is plotted as a function of the molar ratio of added drug to DNA nucleotides. Successive aliquots of 0.5−2 mM drug solutions were added with a calibrated microliter Hamilton syringe into the viscometer containing 2.0 mL of DNA solution (450 μM). The results were corrected for slight changes in DNA concentration during the titration. The inset in panel *a* shows a plot of the concentrations of DNA and NetAmsa at equivalence (the maxima in the plots of flow time *vs* drug/DNA where supercoiling is removed) from three viscometric titrations starting at different DNA concentrations.

Table 1: DNA Binding Properties

	ΔT_m (°C)[a]			Q_{50} (μM)[b]				
	0.1	0.5	1	ethidium	Hoechst	DAPI	ϕ (deg)[c]	R_{drug}[d]
netropsin	12	18	22	3	0.9	1		4.3
SN 16713	4	8	11	1.3	0.45	0.55	18	2.5
amsacrine	1	5	8	3.8	5	5.5	18	6.2
NetAmsa	3	8	10	2	0.7	0.7	9	7.8

[a] Variation in melting temperature (ΔT_m in 0.1 SSC) at D/P ratio of 0.1, 0.5 and 1. [b] Drug concentration (μM) to reduce fluorescence of ethidium, Hoechst 33258, or DAPI bound to DNA. [c] Unwinding angle (ϕ, degrees) with reference to an unwinding angle of 26° for ethidium. [d] Ratio of the reduced dichroism measured in the drug absorption band (310 nm for netropsin and NetAmsa; 450 nm for amsacrine and SN 16713) for the drug bound to DNA and chromatin, $R = [(\Delta A/A)^{drug}{}_{DNA}]/[(\Delta A/A)^{drug}{}_{chromatin}]$ (Bourdouxhe et al., 1992).

et al., 1992b). To test this hypothesis we examined the effect of simultaneously adding netropsin on SN 16713-induced unwinding of DNA (Figure 3). The amount of SN 16713 required to relax fully the supercoiled structure of the plasmid DNA is significantly higher in the presence of an equimolar concentration of netropsin than in its absence. Netropsin reduces by about 25% the apparent unwinding effect of SN 16713. This observation furnishes positive evidence that of the three possibilities, the last one plays at least a contributory part: the lower unwinding observed with the hybrid and with the combination of netropsin and SN 16713 does seem to be due to concomitant overwinding and underwinding produced by the netropsin moiety and the intercalating acridine ring, respectively. Another recent report that minor groove binders modulate DNA supercoiling and in particular that netropsin competes with ethidium bromide for the induction of supercoils on binding to closed circular DNA (Triebel et al., 1994) supports our conclusions.

(B) Circular Dichroism (CD). Binding of the achiral molecule NetAmsa within the chiral environment afforded by the double helical structure in DNA and chromatin leads to an induced optical activity of the DNA-bound hybrid molecules. Figure 4a displays typical CD spectra observed with the hybrid, netropsin, and SN 16713 in the presence of CT DNA. The intercalation of SN 16713 into DNA is manifested by the appearance of a weak negative CD absorption band around 440 nm. Identical negative CD signals in the acridine band, assignable to excitonic coupling between adjacent intercalated molecules, were observed with amsacrine but not with NetAmsa. The conjugate displays intense positive CD signals in the 310 nm absorption band which, by analogy with the CD observed for netropsin, reflect the orientation of the bispyrrole moiety in the minor groove. The disappearance of the negative CD band at 440 nm indicates that the acridine portion of the hybrid molecule, though still intercalated into DNA as judged from the viscometric and ELD data, is oriented differently compared to the acridine moieties of SN 16713 and amsacrine. A simple translation of the intercalated chromophore in the base pair plane (movement from one groove to the other) can produce marked changes in the CD intensity and can even result in reversal of the sign of the CD from negative to positive (Lyng et al., 1991, 1992). The netropsin moiety of the hybrid deeply inserted within the minor groove surely forces the attached acridine ring to adopt a particular orientation within the intercalation site. Here again these results are consistent with the reported fact that netropsin drastically reduces the amplitude of the negative CD signals measured with amsacrine and SN 16713 (Bourdouxhe et al., 1995).

Figure 4c shows the variation of the CD intensity for complexes between the test drugs and chromatin. The presence of histones bound to DNA has no effect on the evolution of the CD for amsacrine and SN 16713. Whether DNA is naked or wrapped around proteins apparently does not influence the intercalation of the acridine ring between base pairs. Conversely, the chromatin structure markedly affects binding in the minor groove, but interestingly, it affects the binding of netropsin and the netropsin moiety of NetAmsa differently. The intensity of the 310 nm CD signal is higher for the netropsin−chromatin complexes than for the netropsin−DNA complexes whereas the opposite is observed with NetAmsa. It seems that the presence of histones facilitates the binding of netropsin to DNA but hinders the binding of the netropsin−amsacrine hybrid ligand. The reduced binding of NetAmsa to chromatin is most likely due to the steric constraints imposed on DNA by the histone complex, constraints which do not allow the two moieties of the hybrid to satisfy fully the geometric ideals

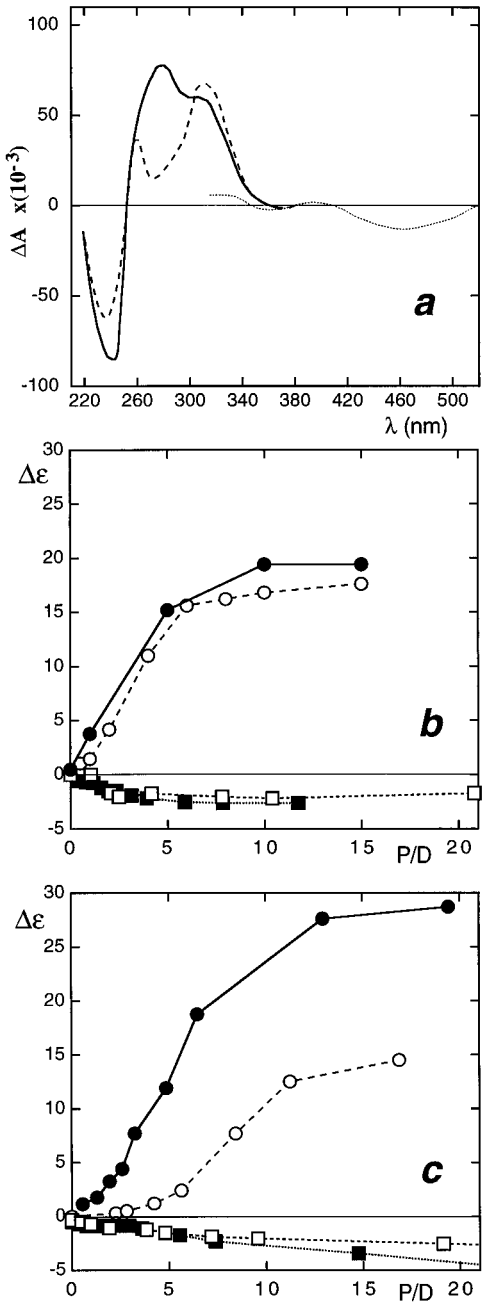

FIGURE 4: Circular dichroism. (a) CD spectra of netropsin (dashed line), NetAmsa (full line), and SN 16713 (dotted line) bound to calf thymus DNA at a P/D ratio of 10. (b and c) Variation in molar circular dichroism $\Delta\epsilon$ (ΔA over drug concentration for 1 cm cell path length) with increasing DNA/drug ratio (b) and chromatin/drug ratio (c) for netropsin (●), NetAmsa (○), amsacrine (■), and SN 16713 (□); $\lambda = 310$ nm for netropsin and NetAmsa, and $\lambda = 440$ nm for amsacrine and SN 16713.

charcteristic of their respective binding modes.

Next we investigated the binding reaction under conditions where the DNA conformation is artificially maintained in a left-handed Z-form so as to determine whether the drug is sensitive to the conformation of DNA. CD measurements were conducted with the alternating copolymer poly(dG-dC)·poly(dG-dC) dissolved in a 1 mM sodium cacodylate buffer containing 60% ethanol (without addition of magnesium ions or other divalent cations) to induce the B→Z transition (Pohl & Jovin, 1972; van de Sande & Jovin, 1982; Bourdouxhe et al., 1995). We examined the effect of netropsin and the hybrid on the Z→B reversion by measuring

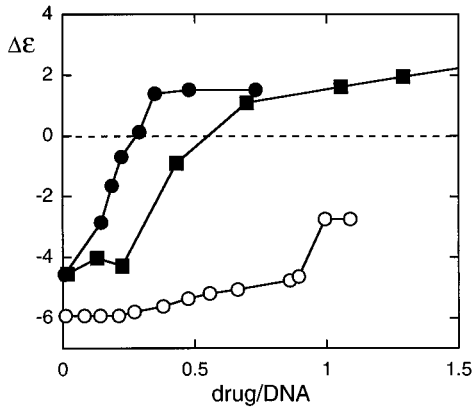

FIGURE 5: Circular dichroism at 290 nm as a function of the molar ratio between netropsin (●) or NetAmsa (○) and poly(dG-dC)·poly(dG-dC). Filled squares (■) show the effect of adding netropsin to a preformed mixture of SN 16713 and poly(dG-dC)·poly(dG-dC) at P/D = 10. The polynucleotide was dissolved in 1 mM sodium cacodylate buffer, pH 6.5, containing 60% ethanol so as to adopt the *Z* conformation.

the intensity of the molar dichroism at 290 nm with increasing drug concentration (Figure 5). Netropsin induces a reversal of the sign of the CD signals from negative to positive, indicating that the Z→B reversion has occurred. It has been known for some time that netropsin induces such conformational changes (Zimmer et al., 1983), but it remains to be determined how netropsin can bind to the B-form of poly(dG-dC)·poly(dG-dC) since the 2-amino group of guanine prevents the drug from inserting into the minor groove (Bailly & Waring, 1995b). It is conceivable that netropsin can bind to the major groove of this GC polymer, as has been proposed for DAPI (Kim et al., 1993). Such major groove binding might account for the low amplitude of the CD signal measured with the B-form of poly(dG-dC)·poly(dG-dC) in the presence of netropsin.

Neither amsacrine nor SN 16713 induces the Z→B reversion under these conditions (Bourdouxhe et al., 1995). When the Z-DNA is preincubated with SN 16713 (at a drug/DNA ratio of 0.1) and then exposed to netropsin, the amount of netropsin required to induce the Z→B transition increases significantly. The reversal of sign occurs at netropsin/DNA ratios of 0.25 and 0.5 in the absence and presence of SN 16713, respectively (Figure 5). With the hybrid ligand, reversion is not observed even at fairly high drug concentrations. It seems that the hybrid molecule either "freezes" the DNA in a Z-like conformation, preventing it from undergoing the Z→B transition, which would indicate an affinity for left-handed DNA, or, notwithstanding its capacity to bind strongly to right-handed B-DNA, it fails to interact with the polynucleotide at all.

(C) Electric Linear Dichroism (ELD). This electrooptical technique provides a convenient tool to investigate whether a ligand is intercalated or bound to the minor groove of DNA. When the drug chromophore is oriented parallel to the plane of the base pairs, as is the case with an intercalated drug, the LD is negative whereas an inclination of the chromophore at about 45° with respect to the orientation axis, as is the case with a minor groove binder, gives rise to a positive LD signal (Houssier, 1981). The ELD spectra of netropsin, amsacrine, SN 16713, and the hybrid bound to DNA and chromatin are shown in Figure 6. The spectrum of the NetAmsa−DNA complex leaves no room for doubt that the

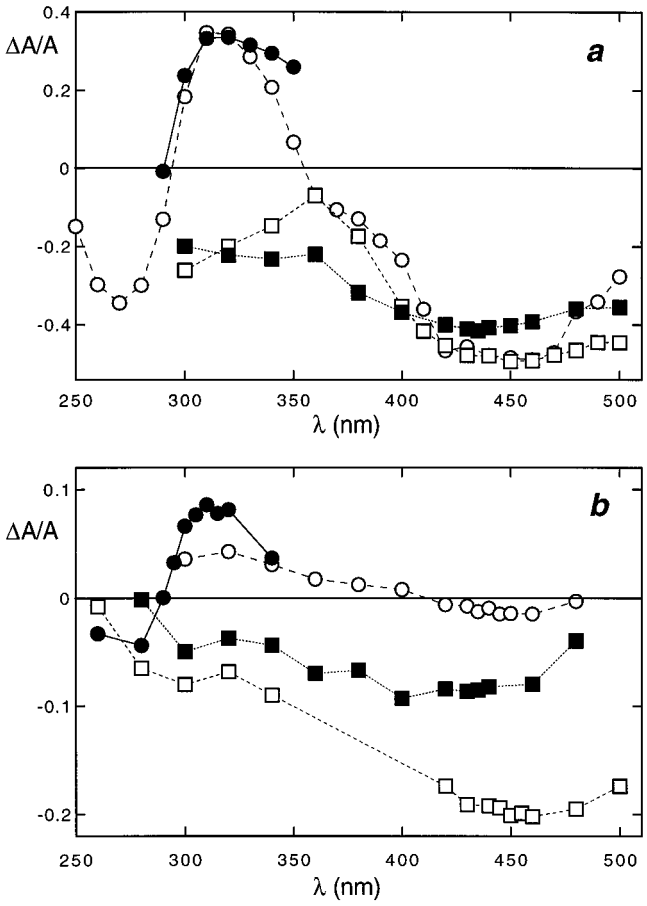

FIGURE 6: Electric linear dichroism. Reduced electric linear dichroism ($\Delta A/A$) spectra of netropsin (●), NetAmsa (○), amsacrine (■), and SN 16713 (□) bound to (a) calf thymus DNA and (b) chromatin. ELD data were recorded in the presence of 100 μM nucleic acids and 10 μM drug, in 1 mM sodium cacodylate buffer, pH 6.5, under a field strength of 13 kV/cm.

hybrid intercalates its acridine chromophore between base pairs and locates its bispyrrole moiety within the minor groove. The positive LD observed with the netropsin−DNA complex is equally intense as that measured with the NetAmsa−DNA complex, and the intensity of the negative LD at 440 nm is identical for all three acridine-containing ligands. Such spectral properties, together with the viscometric and CD data, provide definitive evidence that the objective of creating a hybrid ligand capable of bidentate binding to DNA has been successfully attained. With the first generation of netropsin−anilinoacridine hybrid molecules synthesized (e.g., NetGA, Figure 1), full intercalation of the acridine ring was in most cases precluded owing to the steric constraints produced by the rigid linker between the two DNA-binding functionalities (Bailly et al., 1990). Molecular modeling suggested that a flexible diaminopropyl linker ought to facilitate the bidentate binding process. The prediction was correct as judged from the dichroic and hydrodynamic data reported here.

The situation is different when DNA is coated with histones. The ELD spectrum of the hybrid−chromatin complex displays only weak positive and negative LD at 310 and 440 nm, respectively. Two factors affect the dichroism values observed with drugs bound to chromatin compared to drugs bound to DNA. First, the structural organization of the chromatin in nucleosomes is a factor. Under the low ionic strength conditions required in ELD experiments, chromatin is mostly present as a 10 nm fiber. Because of the compact nucleosome structure, the orientation of the base pairs with respect to the chromatin fiber axis is globally much lower than with naked DNA. The base pairs within the nucleosome are all differently orientated, and consequently, they contribute little, if at all, to the measured dichroism ΔA, but of course, they contribute to the absorbance A. The only base pairs which contribute directly to the LD are those of the internucleosomal linker regions of chromatin which can orientate in the electric field, though not with the same facility as naked DNA. As a result, the reduced dichroism $\Delta A/A$ measured with chromatin is considerably (about 15-fold) lower than that of protein-free DNA. Second, the measured dichroism must reflect any preference of the drug for binding to the linker DNA as opposed to the nucleosomes. The $\Delta A/A$ value measured in the drug absorption band for an intercalating drug homogeneously distributed along the chromatin fiber (equal binding to the linkers and nucleosomes) should be close to the value measured at 260 nm with the drug-free chromatin. Conversely, the $\Delta A/A$ value measured for a ligand bound exclusively to the linker regions should be closer to that measured in the ligand absorption band with protein-free DNA. Thus any preferential localization of a given ligand in the linker regions or the nucleosomes can be estimated by calculating the dichroism ratio $R_{drug} = (\Delta A/A)_{drug,DNA}/(\Delta A/A)_{drug,chromatin}$, i.e., the ratio between the reduced dichroism measured in the drug absorption band in the presence of DNA and the reduced dichroism at the same wavelength in the presence of chromatin. The parameter R_{drug} can vary from 1 for a ligand bound exclusively to the linker regions of chromatin to about 15 for a ligand homogeneously distributed between the linkers and the nucleosomes. A more detailed description of this parameter has been reported previously (Bourdouxhe et al., 1992). The R_{drug} value obtained with netropsin is close to that previously reported for distamycin, as might be expected (Table 1). Both antibiotics bind preferentially to the linker regions of chromatin where the minor groove is more easily accessible. The preference is even more pronounced with the amsacrine-4-carboxamide SN 16713. At first sight, this observation could be attributed to its DNA-threading mode of binding which demands that both grooves of the DNA be readily accessible. It is believed that the threading process takes place primarily during the "breathing motion" of DNA when the two strands are less tightly paired (Denny & Wakelin, 1986). One can therefore conceive that the compact nucleosome structure would not favor the threading process. Surprisingly, the R_{drug} value measured at 310 nm in the netropsin absorption band of the hybrid ligand is much higher than that calculated with amsacrine and is even superior to that obtained with SN 16713 (Table 1). The weak reduced dichroism measured in the acridine band at 450 nm with the hybrid precludes accurate estimation of the R_{drug} parameter at this wavelength. Apparently the conjugate has the capacity to bind to both the linker regions and the nucleosomes. Two hypotheses can be advanced to explain this observation: (i) NetAmsa finds suitable binding sites within the condensed structure of the histone−DNA complex; and (ii) the hybrid decondenses the nucleosome structure so as to render certain DNA sequences available for the threading process. The first hypothesis is rather unlikely since no such effect is observed with SN 16713. The second hypothesis is tested directly in the following section.

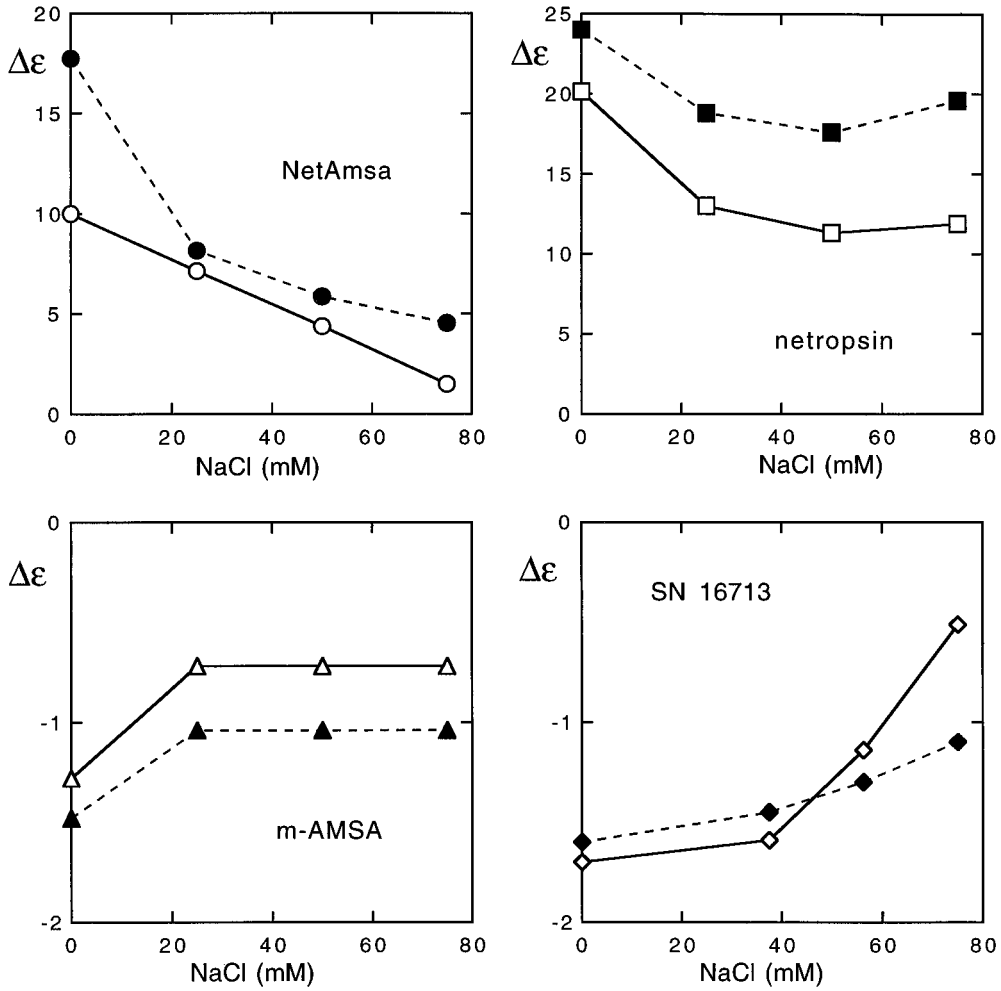

FIGURE 7: Variation in molar circular dichroism $\Delta\epsilon$ (ΔA over drug concentration for 1 cm cell path length) with increasing NaCl concentration for complexes between chromatin and the indicated ligands at P/D ratios of 10 (open symbols) and 50 (filled symbols). $\lambda = 310$ nm for netropsin and NetAmsa, and $\lambda = 440$ nm for amsacrine and SN 16713.

Effects of the Drug on Chromatin Condensation. The results of the CD and ELD experiments showing that the presence of proteins associated with DNA markedly affects the binding of the hybrid ligand prompted us to investigate the effects of the test compounds on chromatin condensation. For that purpose, the salt-jump method described by Hagmar et al. (1992) was used. The structure of the chromatin fiber is dependent on the ionic strength of the solution. With increasing NaCl concentrations, chromatin undergoes a conformational change from a 10 nm fiber to a more condensed 30 nm fiber. Only minor variations of the CD at 260 nm occur during the salt-induced condensation process. Thus, measurements of the variation of the CD in the absorption band of chromatin are too insensitive to determine the effects of drugs on chromatin condensation. However, condensation can be followed indirectly by examining the binding of a drug to chromatin as a function of the salt concentration at different drug/DNA ratios. Figure 7 shows how the CD in the respective absorption bands of the test drugs varies as a function of the salt concentration at two ligand/DNA ratios. In each case the CD amplitude tends to zero as the NaCl concentration increases. Two effects contribute to the decrease of the CD intensity: (i) it is well established that increasing the ionic strength weakens the binding of such cationic drugs; and (ii) the condensation of the chromatin structure consequent upon raising the ionic strength amplifies the steric constraints applicable to chromatin structure, thereby reducing the capacity of the ligands to bind to DNA. For drugs which have no influence on the chromatin condensation process, we expect to observe a nearly identical evolution of the CD signals at DNA/drug ratios of 10 and 50. Such is more or less the case for netropsin and amsacrine but not for the DNA-threading amsacrine-4-carboxamide derivatives SN 16713 and NetAmsa which seem to interfere with the salt-induced mechanism of chromatin condensation. Unlike what is observed with amsacrine, the condensation process is evidently sensitive to the presence of DNA-intercalated SN 16713 molecules since the CD at 450 nm decreases more rapidly at a drug/DNA ratio of 10 than 50. The ELD data ($R_{drug} = 2.5$) indicate that SN 16713 binds preferentially to the linker regions and, therefore, at a P/D ratio of 50 we would expect the proportion of ligand molecules bound to the nucleosomes to be lower than at a P/D ratio of 10. It is possible that SN 16713 affects directly the condensation process to some extent but, given its high selectivity for binding to the linker regions, it is more likely that the pronounced decrease of the CD at a P/D of 10 reflects the predominant release of SN 16713 molecules bound to the nucleosomes, i.e., the fraction of less tightly bound molecules. Conversely, it is much more likely that the salt-induced decrease of the CD at 310 nm observed with the hybrid ligand results chiefly from inhibition of the chromatin condensation process. Indeed, in this case the CD intensity is more sharply reduced

Table 2: Dissociation Constants for Complexes between the Drugs and DNA or Chromatin

	λ^a	drug−DNA[b]		drug−chromatin		
	(nm)	k_1	k_2	k_1	k_2	k_3
netropsin	340	15.6				
amsacrine	450	1.1	33.5	0.76	46.6	
SN 16713	450	0.3	0.5	0.38	3.21	
NetAmsa	340	1.2	2.5			
	450	0.9	4.8	3.8	46.4	156.6
netropsin +	340	15.3				
amsacrine (1:1 ratio)	450	1.2	27.5	2.0	75.5	

[a] Monitoring wavelength (nm). [b] Dissociation constants are expressed in s^{-1}. The stopped-flow kinetic traces of absorbance change *vs* time were fitted satisfactorily with a monoexponential curve for netropsin and with a biexponential curve for amsacrine and SN 16713. With NetAmsa, a two exponential equation was required to fit the curves obtained in the presence of DNA properly, whereas those observed with chromatin could only be fitted satisfactorily by a three exponential equation.

at a DNA/NetAmsa ratio of 50 than at a ratio of 10. This observation, together with the ELD data indicating that the hybrid can bind to both the linkers and the nucleosomes (R_{drug} = 8), strongly suggests that NetAmsa does affect the condensation of chromatin. Unlike its two constituent parts, netropsin and amsacrine, the conjugate apparently interferes with the assembly of histones into the chromatin structure.

Kinetics of the Hybrid−DNA Interaction. Drug−DNA dissociation rate constants were measured by stopped-flow spectrophotometry using the SDS-driven method of Müller and Crothers (1968). For each drug−DNA complex, 8−10 measurements were averaged, and the resulting experimental curve was fitted satisfactorily with a single exponential in the case of netropsin and with two exponentials for the acridine-containing drugs. Derived dissociation rate constants are listed in Table 2. Netropsin is released very rapidly from DNA and the dissociation of amsacrine is even faster. In agreement with previous measurements (Denny & Wakelin, 1986; Bailly et al., 1992c), we found that SN 16713 dissociates much more slowly from DNA. The kinetic stability of the SN 16713−DNA complex is undoubtedly imparted by its carboxamide side chain. Slow dissociation constants characterize the DNA-threading mode of binding to DNA. Combining netropsin and amsacrine at equimolar concentrations does not change their kinetics of dissociation from DNA. In the presence of amsacrine, netropsin still dissociates very rapidly from DNA (and *vice versa*). The situation is very different when the two molecules are covalently linked. Indeed, the dissociation of the hybrid ligand from DNA is considerably slower than that of netropsin or of amsacrine, either individually or in combination. Dissociation constants measured in the netropsin absorption band (at 340 nm) and in the absorption band of the acridine moiety (at 450 nm) are both much lower than those for netropsin and amsacrine, respectively. These observations can only be explained by invoking simultaneous intercalation of the acridine moiety and insertion of the netropsin tail of the hybrid into the minor groove of DNA, but much more elaborate analyses will be required to determine whether the two binding processes are effectively combined into a single binding mode. Nevertheless, the kinetic data furnish persuasive evidence that the desired goal has been achieved: the hybrid ligand behaves as a DNA-threading intercalating agent. The result of attaching an amsacrine-4-carboxamide derivative onto the netropsin moiety has been to increase substantially the residence time of the sequence-reading netropsin element on the double helix.

Is the threading mechanism retained when the DNA is wrapped around proteins? To answer that question, we studied the kinetics of dissociation of the drug from chromatin by stopped-flow spectrophotometry. This time the drug was induced to dissociate by increasing the ionic strength (salt jump) since the SDS-based method is inapplicable with proteins present (chromatin solutions become turbid due to the denaturation of the proteins by the detergent). The dissociation rate constants for various drug−chromatin complexes are given in Table 2. Dissociation of netropsin from chromatin must be extremely rapid since it cannot be detected on the stopped-flow time scale. As with DNA, amsacrine dissociates rapidly from chromatin whereas SN 16713 dissociates much more slowly, suggesting that the threading process is not greatly perturbed by the proteins bound to DNA. By contrast, the netropsin−amsacrine hybrid dissociates a good deal more rapidly from chromatin as predicted from the ELD data (Figure 6b), indicating that the intercalation of the amsacrine moiety of the hybrid into chromatin is inhibited. Competition between NetAmsa and histones for binding to DNA (Figure 7) evidently has a significant effect on the kinetics of hybrid−DNA dissociation.

Sequence-Selective Binding to DNA. To examine the influence of base composition and nucleotide sequence on the binding to DNA of the hybrid and its parent compounds, ELD measurements were performed with a range of natural DNAs and synthetic polynucleotides containing defined repeating sequences. The general base preference of the ligands can be ascertained by comparing the relative values of the dichroism ratio DR. This index refers to the reduced dichroism of the drug−DNA complex measured in the absorption band of the test drug (free of any contribution from DNA) divided by the dichroism of the DNA measured at 260 nm in the absence of drug (see Materials and Methods). Values of DR for any given drug−DNA and drug−polynucleotide complex can be mutually compared independently of the polymer size and are representative of the complex geometry. This method has previously been used to investigate the sequence-dependent interaction of intercalating and minor groove binding drugs (Bailly et al., 1992d) as well as hybrid molecules (Bailly et al., 1994; Colson et al., 1995). Figure 8 illustrates the DR values obtained for complexes between the test drugs and various DNAs and polynucleotides. DR values for netropsin increase with the AT content of the DNA, reflecting its well-recognized AT selectivity. Binding of netropsin to the alternating and nonalternating GC polynucleotides is negligible. The amsacrine-4-carboxamide derivative can bind reasonably well to all types of DNA and polynucleotides. However, the DR values are notably higher with the GC polynucleotides compared to the other types of DNA. This reflects a moderate selectivity for binding to GC sites, as indicated previously by kinetic and footprinting studies (Denny & Wakelin, 1986; Bailly et al., 1992c). With the hybrid molecule, the ELD measurements in the netropsin absorption band (310 nm) and in the acridine absorption band (460 nm) are in agreement that the conjugate binds best to DNA containing mixed AT/GC sequences, particularly the AT-rich DNA from *Clostridium* (which contains 72% A+T

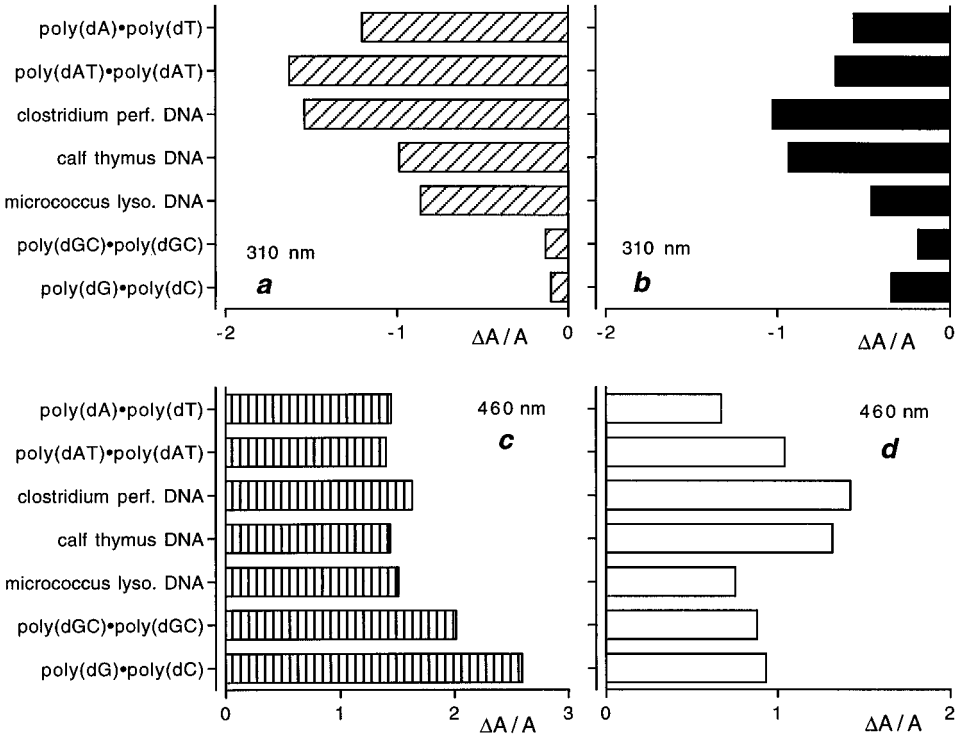

FIGURE 8: Variation of the dichroism ratio (DR) of (a) netropsin, (c) SN 16713, and (b, d) NetAmsa bound to natural DNA and polynucleotides of different base composition. The wavelength of measurement is indicated. For the hybrid, ELD values were measured at 310 nm (b) and 460 nm (d) to monitor the binding of the netropsin and amsacrine moieties, respectively. ELD data were recorded in the presence of 100 μM nucleic acids and 10 μM drug, in 1 mM sodium cacodylate, pH 6.5, under a field strength of 13 kV/cm.

residues). Both moieties of the conjugate are involved in the reaction with pure AT sequences (intense positive reduced dichroism at 310 nm and negative reduced dichroism at 450 nm) but not at GC sites. Indeed, the weak DR values measured at 310 nm with the GC polynucleotides suggest that binding to them does not involve the netropsin portion. Thus with GC polynucleotides the amsacrine moiety intercalates but the netropsin element seems not to be accommodated within the minor groove, no doubt owing to the constraints produced by the exocyclic 2-amino group of guanine residues projecting into it. The 2-amino substituent plays a critical role in the recognition of DNA by many ligands, especially netropsin (Bailly & Waring, 1995b,c). To sum up, although ELD measurements do not provide any direct indication of the relative affinity for different types of DNA, the results suggest that NetAmsa prefers AT sequences. Footprinting studies were performed to test this prediction.

Figure 9 shows the results of a typical DNase I footprinting experiment. The gel and the corresponding differential cleavage plots confirm that netropsin and SN 16713 bind selectively to AT- and GC-rich sequences, respectively, in agreement with previous footprinting studies (Portugal & Waring, 1987; Bailly et al., 1992c; Abu-Daya et al., 1995). Regions protected from DNase I cleavage by the hybrid ligand are confined to the same AT-rich sequences as those detected with netropsin. Complementary DNase I footprinting experiments were carried out with two other restriction fragments, a 265-mer from pBS and the 160 base pair *tyr*T fragment previously used to map binding sites for netropsin and SN 16713 (Bourdouxhe et al., 1995). In each case, the footprints detected with NetAmsa were located exclusively within AT-rich sequences (Table 3); frequently, the DNase I cutting at GC sites was enhanced in the presence of the ligand. Experiments using the transition metal complex MPE·Fe^{II} as a DNA cleaving agent led to the same conclusion (data not shown). Most footprinting experiments indicated that the selectivity of the conjugate for AT sites was weaker than that of netropsin. The strong footprints at GC-rich sequences detected with SN 16713 completely disappeared with the hybrid molecule. These observations support the ELD data presented above, suggesting that NetAmsa exhibits a definite preference for AT-containing regions. They also agree with recent footprinting studies showing that, despite a certain amount of mutual interference, the selective recognition of AT-rich sequences by netropsin tends to dominate the recognition pattern and persists even in the presence of a considerable excess of amsacrine-4-carboxamide (Bourdouxhe et al., 1995). With the different netropsin-based conjugates designed so far it has always been observed that the minor groove binding element imposes its preference for AT-rich sequences.

CONCLUSION

The collective picture which emerges from the variety of experiments reported in this paper is that NetAmsa engages in three modes of interaction with DNA: (1) sequence-specific recognition of the minor groove of the helix via the netropsin moiety, (2) intercalation of the acridine chromophore, and (3) threading of the methanesulfonanilino group into the major groove. It must be acknowledged that, whereas modes 1 and 2 are adequately evidenced by the present results, the exact location of the anilino group has not been directly determined though it would be hard to envisage an alternative model, given the unequivocal evidence for the location of the rest of the hybrid molecule. The kinetic data are certainly fully compatible with the hypothesis that the anilino substituent lies in the major groove

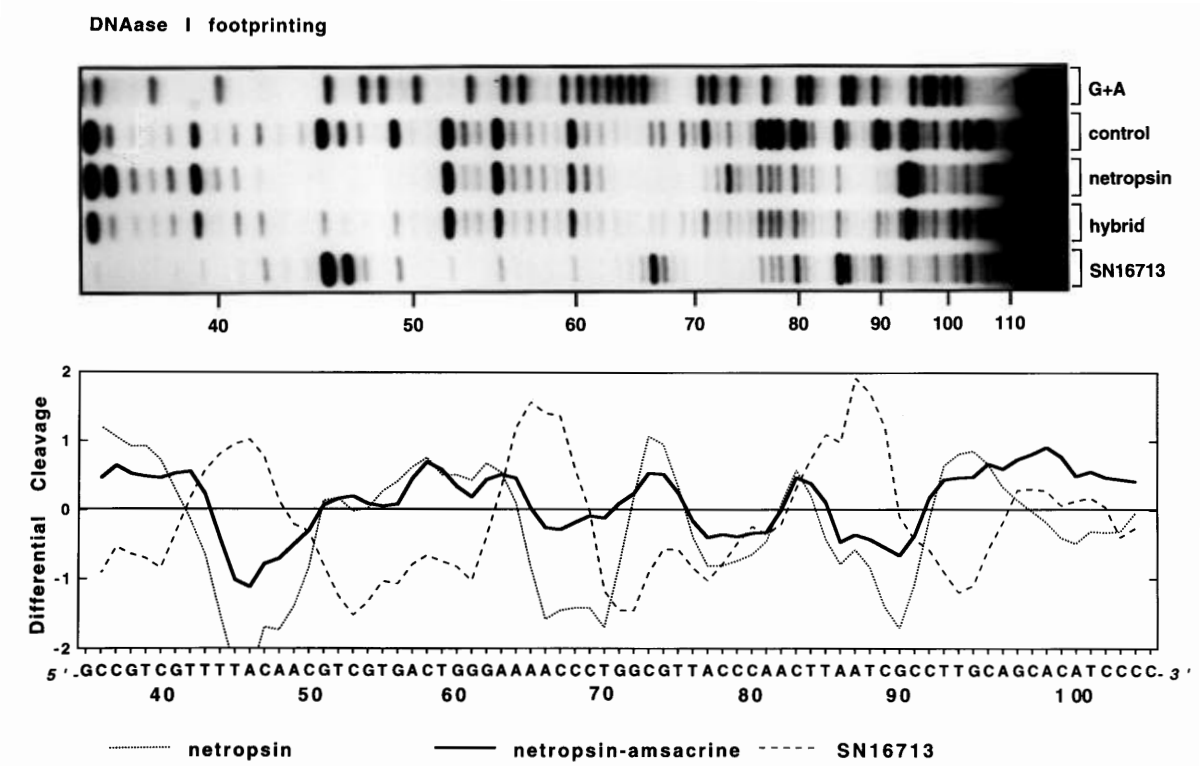

FIGURE 9: DNase I footprinting with the 5′-labeled 117-mer *Pvu*II−*Eco*RI restriction fragment of the plasmid pBS in the presence of netropsin, SN 16713, and the netropsin−amsacrine hybrid (10 μM each). The products of DNase I digestion were resolved on an 8% polyacrylamide gel containing 7 M urea. The control track contained no drug. The track labeled G+A represents a Maxam−Gilbert sequencing marker lane specific for purines. Numbers below the autoradiograph refer to the sequence shown in the differential cleavage diagram where differences in susceptibility of the 117-mer to DNase I cleavage in the presence of netropsin (dotted line), SN 16713 (dashed line), and NetAmsa (solid line) are plotted. Vertical scales are in units of ln (f_a) − ln(f_c), where f_a is the fractional cleavage at any bond in the presence of the drug and f_c is the fractional cleavage of the same bond in the control, given a closely similar extent of overall digestion. Negative values correspond to a ligand-protected site (footprint) and positive values represent enhanced cleavage.

Table 3: Sequences of the *tyr*T and 265-mer DNA Fragments Showing Protection from DNase I Cleavage in the Presence of NetAmsa, Inferred from Differential Cleavage Plots

*tyr*T fragment, from pKMp27	TTTCT, TTACA, TTGATAT, ATAAG, AAAG
265-mer, from pBS	TTTGTT, TTAGT, TAATTTCG, TAATCA

of the double helix. A mechanism involving DNA threading, which requires both the minor groove and the major groove to be simultaneously occupied by the ligand, is also supported by molecular modeling studies undertaken by Dr. Bohdan Waszkowycz (unpublished data). A computer-generated view into the minor groove of his model of NetAmsa bound to the oligonucleotide d(CGCGAATTCGCG)$_2$ is shown in Figure 10. It illustrates how well the spectroscopic and biochemical data reported here correlate with theoretical studies. In the model, the two base pairs at the AT-GC junction are unstacked so as to accommodate the intercalated acridine, and the netropsin tail spans four base pairs in the minor groove. As expected, the methanesulfonanilino substituent protrudes into the major groove. The structure of this hybrid−DNA complex is typical for a threading-type intercalator as has been seen with the anthracycline antibiotic nogalamycin (Egli et al., 1991; van Houte et al., 1993; Smith et al., 1995) and the pluramycins (Hansen & Hurley, 1995, Hansen et al., 1995; Sun et al., 1995) as well as with synthetic drugs such as a naphthalenediimide (Tanious et al., 1991) and certain 2,6-disubstituted anthracene-9,10-dione derivatives (Tanious et al., 1992). There is now ample reason to believe that designing helix-threading combilexins will provide a profitable route for the development of sequence-specific ligands capable of forming stable complexes with DNA (McConnaughie & Jenkins, 1995).

Recent studies have highlighted the role of chromatin in controlling cell growth and function (Wolffe, 1992). In cells, chromatin plays an obvious structural function in as much as it permits a precisely ordered compaction of the genetic material into chromosomes, but it also has functional properties. The realization that transcription of a given gene can actually be assisted by the organization of the DNA into chromatin has rekindled interest in how DNA is packed within the chromatin fibers. For the medicinal chemist, the expansion of knowledge about chromatin has served to reinforce the view that it is of prime importance to investigate drug binding to both DNA and chromatin if we are to comprehend the mechanism of drug action in cells. For these as well as other reasons we have attempted to characterize the binding of the netropsin−amsacrine combilexin to protein-free DNA as well as to DNA assembled into the chromatin structure. Our investigations have revealed that, unlike its constituents netropsin and the amsacrine-4-carboxamide derivative, the hybrid conjugate can interact well with the DNA condensed into nucleosomal structures and can exert a perceptible effect on the salt-induced condensation of DNA. If the effects discovered in the *in vitro* studies described here occur inside cells, the combilexin agent NetAmsa might turn out to be a potent transcription inhibitor endowed with interesting and possibly selective properties. Biological studies are in progress.

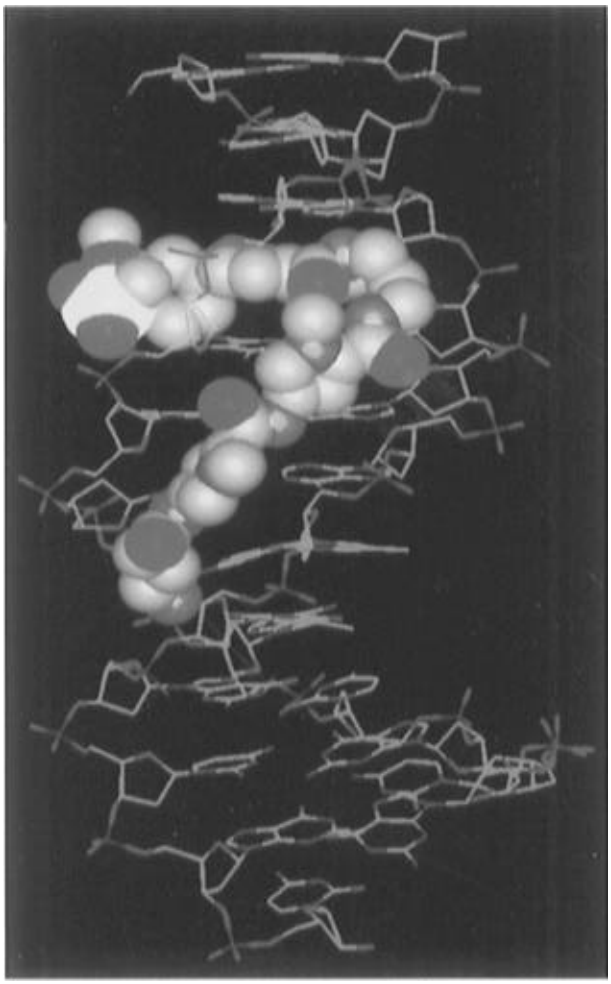

FIGURE 10: View from the minor groove of an energy-minimized model of the complex between NetAmsa and d(GCGCAATTGCGC)$_2$ as calculated by Dr. Bohdan Waszkowycz (Proteus Molecular Design, Macclesfield, U.K). The molecular model illustrates the threading of the hybrid through the double helix so as to occupy both the minor and major grooves. The netropsin moiety of the hybrid lies in the minor groove of the AATT central core, the acridine ring is intercalated between the last A·T base pair and the adjacent C·G base pair, and the methanesulfonanilino group resides in the major groove.

ACKNOWLEDGMENT

The authors thank Pr. Jean-Pierre Hénichart for assistance on the work on hybrid molecules, Pr. William Denny for providing the amsacrine-4-carboxamide derivative SN 16713, and Dr. Bohdan Waszkowycz for the molecular modeling.

REFERENCES

Abu-Daya, A., Brown, P. M., & Fox, K. R. (1995) *Nucleic Acids Res. 23*, 3385−3392.

Baguley, B. C., Denny, W. A., Atwell, G. J., & Cain, B. F. (1981) *J. Med. Chem. 24*, 170−177.

Bailly, C., & Hénichart, J. P. (1991) *Bioconjugate Chem. 2*, 379−393.

Bailly, C., & Hénichart, J. P. (1994) in *Molecular Aspects of Anticancer Drug−DNA Interactions* (Neidle, S., & Waring, M. J., Eds) Vol. 2, pp 162−196, Macmillan, London.

Bailly, C., & Waring, M. J. (1995a) *J. Biomol. Struct. Dyn. 12*, 869−898.

Bailly, C., & Waring, M. J. (1995b) *Nucleic Acids Res. 23*, 885−892.

Bailly, C., & Waring, M. J. (1995c) *J. Am. Chem. Soc. 117*, 7311−7316.

Bailly, C., Pommery, N., Houssin, R., & Hénichart, J. P. (1989) *J. Pharm. Sci. 78*, 910−917.

Bailly, C., Helbecque, N., Hénichart, J. P., Colson, P., Houssier, C., Rao, K. E., Shea, R. G., & Lown, J. W. (1990) *J. Mol. Recognit. 3*, 26−35.

Bailly, C., Collyn-d'Hooghe, M., Lantoine, D., Fournier, C., Hecquet, B., Fossé, P., Saucier, J. M., Colson, P., Houssier, C., & Hénichart, J. P. (1992a) *Biochem. Pharmacol. 43*, 457−466.

Bailly, C., OhUigin, C., Houssin, R., Colson, P., Houssier, C., Rivalle, C., Bisagni, E., Hénichart, J. P., & Waring, M. J. (1992b) *Mol. Pharmacol. 41*, 845−855.

Bailly, C., Denny, W. A., Mellor, L., Wakelin, L. P. G., & Waring, M. J. (1992c) *Biochemistry 31*, 3514−3524.

Bailly, C., Hénichart, J. P., Colson, P., & Houssier, C. (1992d) *J. Mol. Recognit. 5*, 155−171.

Bailly, C., Leclère, V., Pommery, N., Colson, P., Houssier, C., Rivalle, C., Bisagni, E., & Hénichart, J. P. (1993) *Anti-Cancer Drug Des. 8*, 145−164.

Bailly, C., Michaux, C., Colson, P., Houssier, C., Sun, J. S., Garestier, T., Hélène, C., Hénichart, J. P., Rivalle, C., Bisagni, E., & Waring, M. J. (1994) *Biochemistry 33*, 15348−15364.

Bartkowiak, J., Kapuscinski, J., Melamed, M. R., & Darzynkiewicz, Z. (1989) *Proc. Natl. Acad. Sci. U.S.A. 86*, 5151−5154.

Bishop, J. M. (1987) *Science 235*, 305−311.

Bourdouxhe, C., Colson, P., Houssier, C., Sun, J.-S., Montenay-Garestier, T., Hélène, C., Rivalle, C., Bisagni, E., Waring, M. J., Hénichart, J. P., & Bailly, C. (1992) *Biochemistry 31*, 12385−12396.

Bourdouxhe, C., Colson, P., Houssier, C., Hénichart, J. P., Waring, M. J., Denny, W. A., & Bailly, C. (1995) *Anti-Cancer Drug Des. 10*, 131−154.

Chaires, J. B. (1990) *Biophys. Chem. 35*, 191−202.

Chaires, J. B., Dattagupta, N., & Crothers, D. M. (1985) *Biochemistry 24*, 260−267.

Chen, A. Y., & Liu, L. F. (1994) *Annu. Rev. Pharmacol. Toxicol. 34*, 191−218.

Chen, Y.-H., & Lown, J. W. (1994) *J. Am. Chem. Soc. 116*, 6995−7005.

Clark, D., Reitman, M., Studitsky, V., Chung, J., Westphal, H., Lee, E., & Felsenfeld, G. (1993) *Cold Spring Harbor Symp. Quant. Biol. 58*, 1−6.

Colson, P., Bailly, C., & Houssier, C. (1996) *Biophys. Chem. 58*, 125−140.

Denny, W. A., & Wakelin, L. P. G. (1986) *Cancer Res. 46*, 1717−1721.

Denny, W. A., & Wakelin, L. P. G. (1990) *Anti-Cancer Drug Des. 5*, 189−200.

Egli, M., Williams, L. D., Frederick, C. A., & Rich, A. (1991) *Biochemistry 30*, 1364−1372.

Feigon, J., Denny, W. A., Leupin, W., & Kearns, D. R. (1984) *J. Med. Chem. 27*, 450−465.

Felsenfeld, G. (1992) *Nature 355*, 219−224.

Fossé, P., René, B., Saucier, J. M., Hénichart, J. P., Waring, M. J., Colson, P., Houssier, C., & Bailly, C. (1994) *Biochemistry 33*, 9865−9874.

Geierstanger, B. H., Mrksich, M., Dervan, P. B., & Wemmer, D. E. (1994) *Science 266*, 646−650.

Hagmar, P., Marquet, R., Colson, P., Kubista, M., Nielsen, P., Nordèn, B., & Houssier, C. (1989) *J. Biomol. Struct. Dyn. 7*, 19−33.

Hagmar, P., Pierrou, S., Nielsen, P., Nordén, B., & Kubista, M. (1992) *J. Biomol. Struct. Dyn. 9*, 667−679.

Hansen, J. C., & Ausio, J. (1992) *Trends Biochem. Sci. 17*, 187−191.

Hansen, M., & Hurley, L. (1995) *J. Am. Chem. Soc. 117*, 2421−2429.

Hansen, M., Yun, S., & Hurley, L. H. (1995) *Chem. Biol. 2*, 229−240.

Houssier, C. (1981) in *Molecular Electro-Optics* (Krause, S., Ed.) pp 363−398, Plenum Publishing Corp., New York.

Houssier, C., & O'Konski, C. T. (1981) in *Molecular Electro-Optics* (Krause, S., Ed.) pp 309−339, Plenum Publishing Corp., New York.

Hurley, L. H. (1988) *Trends Pharmacol. Sci. 9*, 402−407.

Hurley, L. H. (1989) *J. Med. Chem. 32*, 2027−2033.

Kapuscinski, J., & Darzynkiewicz, Z. (1984) *Proc. Natl. Acad. Sci. U.S.A. 81*, 7368−7372.
Kapuscinski, J., & Darzynkiewicz, Z. (1986) *Proc. Natl. Acad. Sci. U.S.A. 83*, 6302−6306.
Kim, S. K., Eriksson, S., Kubista, M., & Nordèn, B. (1993) *J. Am. Chem. Soc. 115*, 3441−3447.
Kopka, M. L., & Larsen, T. A. (1992) in *Nucleic Acid Targeted Drug Design* (Propst, C. L., & Perun, T. J., Eds.) pp 303−374, Marcel Dekker, Inc., New York.
Low, C. M. L., Drew, H. R., & Waring, M. J. (1984) *Nucleic Acids Res. 12*, 4865−4877.
Lown, J. W. (1995) *Drug Dev. Res. 34*, 145−183.
Lyng, R., Rodger, A., & Nordén, B. (1991) *Biopolymers 31*, 1709−1720.
Lyng, R., Rodger, A., & Nordén, B. (1992) *Biopolymers 31*, 1201−1214.
McConnaughie, A. W., & Jenkins, T. C. (1995) *J. Med. Chem. 38*, 3488−3501.
Müller, W., & Crothers, D. M. (1968) *J. Mol. Biol. 35*, 251−290.
Nielsen, P. E. (1991) *Bioconjugate Chem. 2*, 1−12.
Plouvier, B., Houssin, R., Hecquet, B., Colson, P., Houssier, C., Waring, M. J., Hénichart, J. P., & Bailly, C. (1994) *Bioconjugate Chem. 5*, 475−481.
Pohl, F. M., & Jovin, T. (1972) *J. Mol. Biol. 67*, 375−396.
Portugal, J., & Waring, M. J. (1987) *Eur. J. Biochem. 167*, 281−289.
Powis, G., & Workman, P. (1994) *Anti-Cancer Drug Des. 9*, 263−277.
Ralph, R. K., Judd, W., Pommier, Y., & Kohn, K. W. (1993) in *Molecular Aspects of Anticancer Drug−DNA Interactions* (Neidle, S., & Waring, M. J., Eds.) pp 1−95, Macmillan, London.
René, B., Fossé, P., Khélifa, T., Jacquemin-Sablin, A., & Bailly, C. (1996) *Mol. Pharmacol.* (in press).
Révet, B. M., Schmir, M., & Vinograd, J. (1971) *Nat. New Biol. 229*, 10−13.
Riou, J. F., Grondard, L., Naudin, A., & Bailly, C. (1995) *Biochem. Pharmacol. 50*, 424−428.
Schröter, H., Maier, G., Ponsting, H., & Nordheim, A. (1985) *EMBO J. 4*, 3867−3872.
Smith, C. K., Davies, G. J., Dodson, E. J., & Moore, M. H. (1995) *Biochemistry 34*, 415−425.
Snounou, G., & Malcolm, A. D. B. (1983) *J. Mol. Biol. 167*, 211−216.
Sun, D., Hansen, M., & Hurley, L. H. (1995) *J. Am. Chem. Soc. 117*, 2430−2440.
Tanious, F. A., Jenkins, T. C.., Neidle, S., & Wilson, W. D. (1992) *Biochemistry 31*, 11632−11640.
Triebel, H., Bär, H., Walter, A., Burckhardt, G., & Zimmer, Ch. (1994) *J. Biomol. Struct. Dyn. 11*, 1085−1105.
Van de Sande, J. H., & Jovin, T. M. (1982) *EMBO J. 1*, 115−126.
van Houte, L. P. A., van Garderen, C. J., & Patel, D. J. (1993) *Biochemistry 32*, 1667−1674.
Wakelin, L. P. G., & Waring, M. J. (1980) *J. Mol. Biol. 144*, 183−214.
Wakelin, L. P. G., Chetcuti, P., & Denny, W. A. (1990) *J. Med. Chem. 33*, 2039−2044.
Wang, J. C. (1974) *J. Mol. Biol. 89*, 783−801.
Waring, M. J. (1970) *J. Mol. Biol. 54*, 247−279.
Waring, M. J. (1976) *Eur. J. Cancer 12*, 995−1001.
Waring, M. J., & Henley, S. M. (1975) *Nucleic Acids Res. 2*, 567−586.
Wells, R. D., Larson, J. E., Grant, R. C., Shortle, B. E., & Cantor, C. R. (1970) *J. Mol. Biol. 54*, 465−497.
Wilson, W. D., & Tanious, F. A. (1994) in *Molecular Aspects of Anticancer Drug−DNA Interactions* (Neidle, S., & Waring, M. J., Eds.) Vol. 2, pp 243−269, Macmillan, London.
Wolffe, A. (1992) *Chromatin. Structure and Function*, Academic Press, London.
Zimmer, C., Marck, C., Guschlbauer, W. (1983) *FEBS Lett. 154*, 156−160.

BI9528098